ELSEVIER

Biophysical Chemistry 80 (1999) 103–118

Biophysical Chemistry

www.elsevier.nl/locate/bpc

Low doses of α- and γ-radiation enhance DNA thermal stability

A.G. Georgakilas[a], E.G. Sideris[a], L. Sakelliou[b], C.A. Kalfas[c,*]

[a] *NCSR Demokritos, Institute of Biology, Agia Paraskevi 153 10, Athens, Greece*
[b] *University of Athens, Physics Department, Panepistimioupolis, Ilisia, 157 71, Athens, Greece*
[c] *NCSR Demokritos, Institute of Nuclear Physics, Agia Paraskevi 153 10, Athens, Greece*

Received 20 June 1998; received in revised form 10 March 1999; accepted 28 April 1999

Abstract

Isolated calf thymus DNA in buffered solutions has been exposed to 0–150 Gy of α- and γ-radiation. The effects of α- and γ-radiation on the thermal stability and electrophoretic mobility of the DNA molecules have been studied by UV spectroscopic 'melting' and Pulsed Field Gel Electrophoresis (PFGE), respectively. The observed thermal denaturation parameters were fitted to the energy propagation descriptive model. The experimental results for the samples exposed to relatively low (*low*) doses indicate an increased thermal stability and a reduced mobility over that of the controls. The expected overall degradation of the DNA molecules was confirmed for the samples exposed to *high* doses. Our results are in good agreement with the predictions of the energy propagation model, which now is also tested in the *low* dose region and for an additional type of ionising radiation (α-particles). Our findings are consistent with conformational changes at *low* doses resulting in a DNA form characterised by localised alterations, which affect the energy flow along the DNA molecule.

Keywords: DNA; Thermal stability; Ionising radiation; *Low* doses; Energy flow

1. Introduction

In a recently published paper [1] a model of the thermal transition of macromolecular DNA was described and tested for samples exposed to a wide range of relatively high doses of γ-radiation. The possible dependence of all the derived parameters (related to thermal stability, T_M, number of disrupted base pairs/grad, $\sqrt[N+1]{c}$, and energy propagation along the DNA molecule, N) on the type of ionising radiation and the radiation-induced changes of the DNA structure had to be further investigated.

It is known [2–5] that exposure of the DNA

* Corresponding author. Tel.: +30-1-6503-528; fax: +30-1-6511-215
E-mail address: kalfas@mail.demokritos.gr (C.A. Kalfas)

0301-4622/99/$ - see front matter
PII: S0301-4622(99)00064-2

molecule to any kind of ionising radiation may result in a single or multiple lesions such as base or sugar damage, alkali labile sites, cross-linking, single strand breaks (SSBs) and double strand breaks (DSBs), the latter considered as the most lethal lesion for the cell in vivo and in vitro [4,6]. The study of the possible effects of relatively low (*low*) doses of ionising radiation on isolated DNA in solution has been restricted mainly to gamma rays as reviewed in [7]. Although no definite conclusions about the possible alterations occurring on the DNA double helix at *low* doses and *low* dose rates can be drawn so far, it seems possible that the radiation effects are restricted to conformational changes of the DNA double helix. They would result from localised damages mainly on the sugar phosphate backbone and from possible changes of DNA stacking as stated in a review paper by Wheeler [7]. It has been shown for double stranded oligonucleotides that any accidental change on the B-conformation of the DNA double helix such as variation of twist angles or of base conformation leads to changes in the counterion distribution around the helix [8]. This affects the counterion uptake and release and has significant effects on the stacking between the neighbouring bases of each strand. Any change in base stacking will affect, positively or negatively, helix stability [8,9]. On the other hand it has been shown, by applying DNA melting measurements on γ-irradiated polynucleotides in buffered solutions, that helix thermal stability seems to have a marked dependence on the bases involved in the structure [10,11]. Ward and Urist [10] and later Rafi et al. [12] explained the initial 'lag' in base destruction, observed at *low* doses, by suggesting that at relative *low* doses the double helical structure, which still exists partially intact, protects bases which lie in the interior and only when *high* doses cause a breakdown of the B-form, base destruction occurs. The fact that at *low* doses single strand breaks, SSBs, dominate over double strand breaks, DSBs [3,13], has led many researchers to the conclusion that at *low* doses the reduced formation of SSBs and the destruction of nearby base molecules permits sections of the double helix to un-zip [14]. Conformational changes of the B-DNA structure induced by a relatively small number of SSBs (mainly local opening and destabilization) are suggested [7].

The stability of the DNA molecule depends on several parameters, mainly base composition, ionic strength and molecule size. It is known [15] that the most stable regions are the G-C regions, thus DNA molecules with higher G-C content show increased thermal stability, as revealed with UV 'melting'. The dependence of the DNA double helix to single coil thermal transition (melting) temperature, T_M, on G-C content and salt concentration are sufficiently described in a simple equation given by Schildkraut and Lifson [16]. The molecular size dependence of the melting temperatures is described in a formula given by Britten et al. [17] but only for a certain range of ionic strength. Concerning the radiation effects on the thermal stability of DNA, only a few results have been published so far [18–21]. All of them confirm that *high* doses of γ- or X-rays result in an decreased helix stability due to the accumulating strand breaks and to the consequent increasing disruption of DNA base stacking and hydrogen bonding. This instability is revealed by the monotonous decrease of the T_M values as a function of dose. Very limited data exist on *low* dose (< 10 Gy) effects on the thermal stability of DNA [20–22]. Uyesugi and Trumbore [20,21], attribute the observed increased stability of samples exposed to *low* doses to a statistical important radiation-induced (metal-ion assisted) B- to Z-DNA conversion. However, concerning α-radiation, no relevant data are available in the literature.

The existing models for DNA thermal denaturation might be divided in two major groups. The models of the first group consider the molecule as a static one-dimensional structure. All the predictions are based on the statistical confrontation of the melting behaviour of a certain DNA region and on the fact that the A-T rich regions melt earlier than the G-C regions [23,24]. These models are essentially Ising-like, where a base pair is considered as a two-state system, which is either closed or open. Approaches like these cannot reproduce the full dynamics of the denaturation, which is a highly cooperative phenomenon. In the second group, several dynamic approaches exist

for describing the thermal transition of a DNA molecule. Some of them are limited to the description of simple DNA systems of low molecular weight [25] or valid only for certain temperature regions (mainly the pre-melting region). The second-order self-consistent phonon theory results deviate significantly from the experimental ones, pointing to the fundamental role of non-linear processes in DNA denaturation [26]. Most of these investigations have focused on the formation and the propagation of solitary wave excitations along the double helix. On the other hand, no other attempts have been made to produce a comprehensive theory capable of correlating thermal transition phenomena with radiation effects based on experimental results.

In this paper, we test the model proposed by Kalfas et al. [1] for two different types of ionizing radiation, γ-(photon radiation) and α-(particle radiation) and in various irradiation conditions including the *low* dose range. Analytical results about the region of *low* doses are presented. The radiation effects at *low* and *high* doses on the apparent molecular size seem to correlate with all the parameters introduced in the model. Furthermore, an effort is made to explain the enhanced stability at low doses revealed in our data.

2. Materials and methods

2.1. Preparation of DNA samples

The experimental work was performed using buffered aqueous solutions of calf thymus DNA (Type I) from Sigma Chemical Co, repeatedly deproteinised. For the preparation of the DNA solutions exposed to α- and γ-radiation, 16 mg of pure DNA were dissolved in 1 ml of $0.1 \times$ SSC buffer ($0.1 \times$ saline sodium citrate: 1.55×10^{-2} M sodium chloride, 1.5×10^{-3} M sodium citrate) for 24 h in 4°C at neutral pH. The concentration of the solutions was 5×10^{-2} M in DNA-(P) as determined spectrophotometrically measuring the A_{266} UV-absorbance at room temperature. Aliquots of these solutions (7-μl volume) were α- and γ-irradiated at room temperature. Immediately after the irradiations, the samples were diluted in $0.01 \times$ SSC to a final concentration of 7×10^{-5} M in DNA-(P). All buffers were dearated before use applying a moderate vacuum for 45 min.

2.2. DNA UV melting

All the DNA thermal transition measurements were carried out at the concentration of 7×10^{-5} M DNA-(P). The thermal double helix to single coil transition (denaturation) and the reverse transition, i.e. the coil-to-helix transition (renaturation) were studied by monitoring the A_{266} UV-absorbance of the dearated solutions while increasing or decreasing the temperature at a rate of 1°C/min in the temperature range 25–90°C [42]. The above rate offers a satisfactory alignment of complementary strands while in the renaturation process. On the other hand, it minimises the probability of generating single strand breaks (SSBs) in DNA due to the extended exposure of the sample to high temperatures. To ensure that the renaturation process is not dependable and kinetically controlled — under the conditions applied here (DNA size, concentration and ionic strength) — by the chosen rate of 1°C/min, we performed a series of additional measurements applying a lower rate of 0.5°C/min for three characteristic doses (0, 3.9 and 150 Gy of γ-rays). Our results didn't show any statistically important differentiation except for the dose of 150 Gy where the renaturation capability of the irradiated DNA samples was found to be ~12% reduced due to the expected (as mentioned above) increase in the number of SSBs. The changes in UV-absorbance at 266 nm, A_{266} vs. temperature, were recorded using a GBC 918 UV-VIS spectrophotometer with a fully automated Peltier temperature controller of the multiple cell holder, on line with a PC. For the fitting process applied to the sigmoidal thermal transition curves of the DNA samples, the MINUIT code [27] was used.

2.3. Irradiation of DNA samples

The γ-irradiation of the DNA samples were performed with a ^{60}Co source from Atomic

Canada Ltd. The dose rate at the irradiation position was (6.4 ± 0.2) cGy/s. For α-irradiation, a simple exposure apparatus was constructed, which allows uniform irradiation of the liquid samples at various dose-rates and assures reliable dosimetry [28]. A ^{241}Am surface source (Amersham) of 25 MBq nominal activity emitting in vacuum, was used. The liquid samples were placed on 7-μm Mylar foil, stretched over the exit window. For α-dosimetry the experimental procedure described by Zarris et al. was followed. The α-dose rate at the Mylar–liquid interface was (0.55 ± 0.04) cGy s^{-1} [22].

2.4. DNA size determination

The average apparent size (and mean apparent MWs) of the control DNA samples and those exposed to ionising irradiation were estimated on the basis of their electrophoretic mobility during PFGE following the method previously described [29]. Briefly, 5–10 μg of DNA embedded in 1% low melting agarose (Sigma Chemical Co.) plugs were loaded per gel lane. The 0.8% agarose gels (Sigma Chemical Co.) were run in $0.25 \times$ TBE electrophoretic buffer ($1 \times$ TBE: 90 mM Tris, 88 mM boric acid and 2 mM EDTA, pH = 8), 180–120 V (5.7 V/cm logarithmically changing) with a switch time changing from 60 to 10 s, over 15 h at a maximum of 13°C according to the manufacturer of the sited Rotaphor Type V apparatus (Biometra GmbH). Two micrograms of λ *Hind III* DNA marker (New England Biolabs Co.) also embedded in 1% low melting agarose plugs, were loaded in each gel for size calibration. After running, the gels were stained for 30 min with 10 μg/ml ethidium bromide in 0.1 M ammonium acetate buffer (pH = 7.5) and destained by immersing them for 1 h in the same buffer without ethidium bromide. The gels were then photographed using short-length, UV irradiation. The intensities of the fluorescence of the DNAs in each lane were detected by scanning the films' negatives (Polaroid 665) in 600×600 dpi resolution, using an Epson GT-8000 Scanner. The information from each gel picture was then digitalised (256 different gray values are attached to different fluorescence intensities) and used with software specially developed to measure the intensity distribution of each lane. Using a multiple Gaussian fit, for the intensity distribution of each lane, the corresponding apparent average MWs, in kilobase pairs, were estimated for the DNA samples on the basis of the intensity distribution profile of the marker.

3. Results and discussion

3.1. Irradiation and melting curves

DNA samples were exposed to a wide range of doses of α- and γ-radiation (0–150 Gy). The effects of γ- and α-irradiation in the thermal transition of DNA samples are presented in Figs. 1 and 2, respectively. Each series of these experiments was carried out within the same day to minimise the effects of instrumental instability. In these figures the corresponding thermal transition (denaturation) and the reverse transition (renaturation) experimental data with their fitted curves and their first derivatives are shown. The experimental data were fitted according to the proposed by Kalfas et al. [1] relationship between the absorbance $A(\theta)$ and the temperature θ:

$$A(\theta) = A_{st} + A_u\left(1 - e^{-\frac{c(\theta-\theta_0)^{N+1}}{N+1}}\right) \quad \text{for } \theta > \theta_0 \tag{1}$$

where $A(\theta)$ is the A_{266} absorbance at a given temperature θ; A_{st}, is the A_{266} of the tight double helical form at the threshold temperature θ_0, for the helix to coil transition; A_u, is the increase of A_{266} corresponding to denatured DNA, i.e. the cause of the hyperchromic effect; N is the exponent related to the possible paths of energy propagation along the DNA macromolecule and c is a proportionality constant. Based on the above model, melting (sigmoidal) curves of the expected $A(\theta)$ values were fitted to the experimental data. All the model parameters were calculated using Eq. (1). The experimental data and the best-fit curves are presented in Fig. 1 for γ-irradiation and Fig. 2 for α-irradiation, respectively. A good

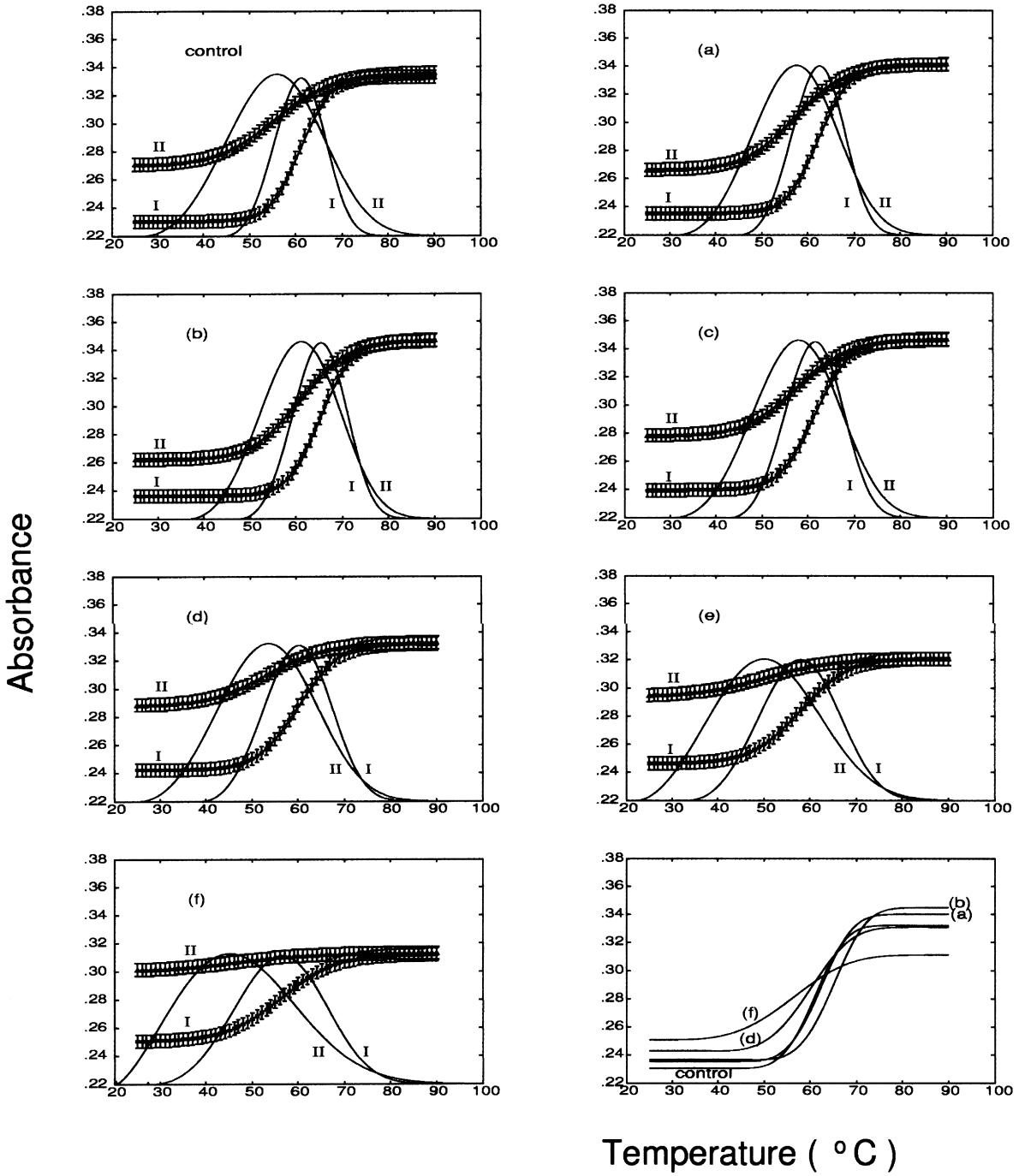

Fig. 1. DNA 'melting' profiles for γ irradiation: **I** *denaturation* and **II** *renaturation curves*. The solid lines for each figure correspond to the best-fit curves of the experimental data and their first derivatives, respectively for the non-irradiated DNA samples (control) and for the DNA samples irradiated with 1.6 (a), 3.9 (b), 8.7 (c), 37 (d) 74 (e) and 150 (f) Gy of γ-rays. An overlay of the fitted curves for selected doses is presented in (g). The error bars correspond to the mean ±S.D.

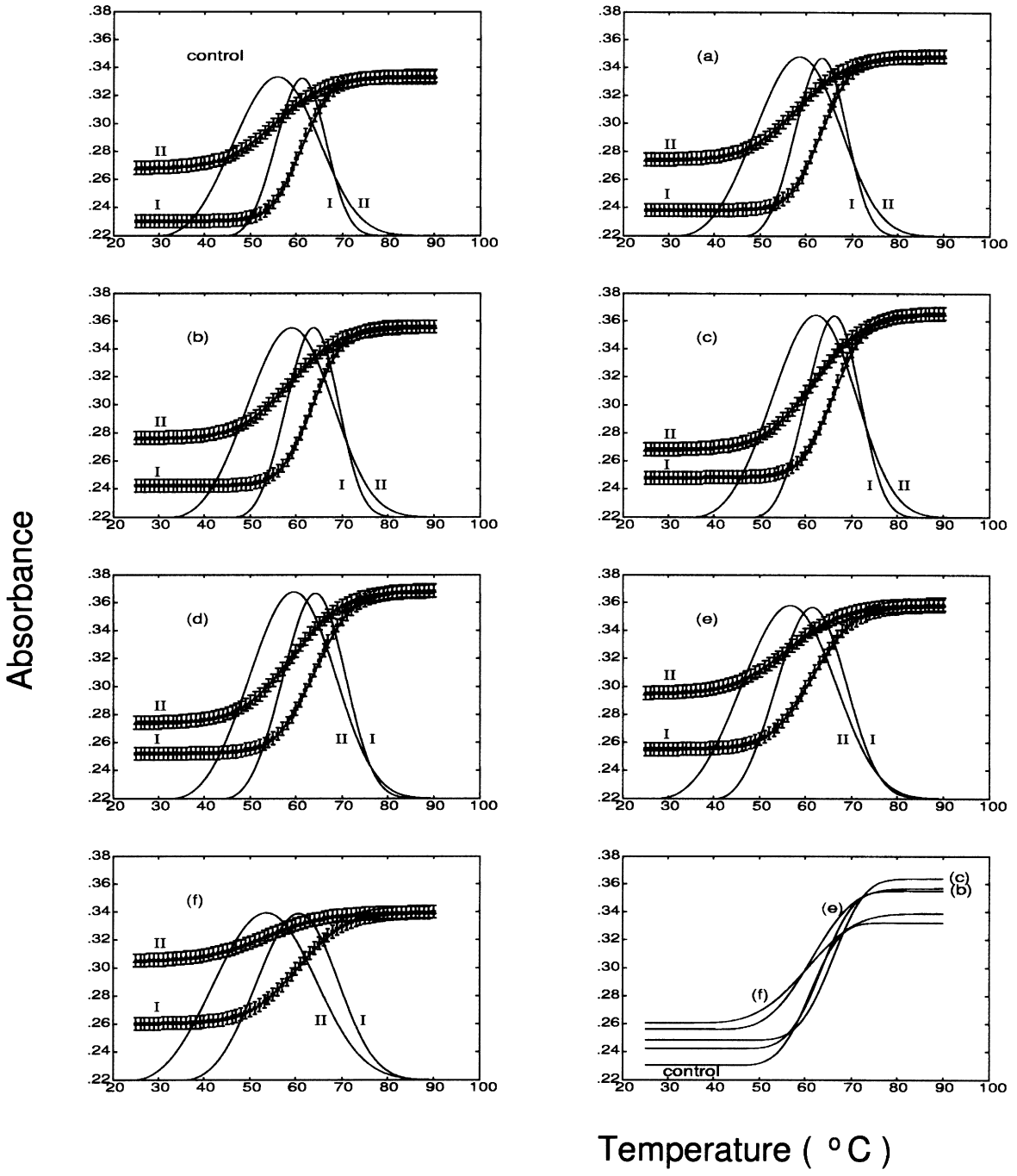

Fig. 2. DNA 'melting' profiles for α irradiation: **I** *denaturation* and **II** *renaturation curves*. The solid lines for each figure correspond to the best-fit curves of the experimental data and their first derivatives, respectively for the non-irradiated DNA samples (control) and for the DNA samples irradiated with 0.8 (a), 4 (b), 12 (c), 9 (d), 56 (e) and 100 (f) Gy of α-particles. An overlay of the fitted curves selected doses is presented in (g). The error bars correspond to the mean ±S.D.

agreement between theoretical and experimental values of $A(\theta)$ for both for γ- and α-data has been found as it can be seen in Fig. 1a–f and Fig. 2a–f. Selected melting overlays can be seen in Figs. 1g and 2g.

The study of the transitions (melting and reverse) at low temperatures (25°C) for the irradiated samples and the control revealed a slight increase at the A_{266} as a function of dose. This finding can be attributed to the fact that even at *low* doses, certain sections of the DNA may be altered. These alterations may include loose ends caused by strand breaks or any other kind of damage (sugar or base damage) directly correlated with changes in base stacking [4]. Some variations for this phenomenon have been reported previously [18], when calf thymus DNA was irradiated with γ- or X-rays. On the other hand, for high temperatures, a decrease in A_{266} is observed with the increase of dose. This decrease can be attributed to extended base pair destruction with a resulting loss of chromophores at 266 nm [4]. A higher decrease is observed for the samples exposed to *high* doses of γ-rays. This is expected for γ-rays since it has been shown that the total strand breaks induced by such doses are much higher for γ-rays than α-particles [30]. The above fact would result to higher DNA degradation and destabilisation, something which has been confirmed from our present results (see Section 3.2).

At the *low* dose region (0–6 Gy for γ-irradiation and 0–32 Gy for α-irradiation) the higher thermal stability of the samples is revealed through a shift of the melting curves towards higher temperatures (the increase of A_{266} starts at significantly higher temperatures) and a higher reversibility. This higher reversibility is indicative of an increase between complementary base pairs which is preserved (up to an extent) even after denaturation and therefore facilitates the reassociation of the two strands during the renaturation process. The shift of the transition curves can be also seen in the overlay Figs. 1g and 2g and also in Fig. 3 and Fig. 4, where an overlay of the first derivatives of selected melting curves is plotted as a function of temperature. From the first derivative analysis one can make two significant observations:

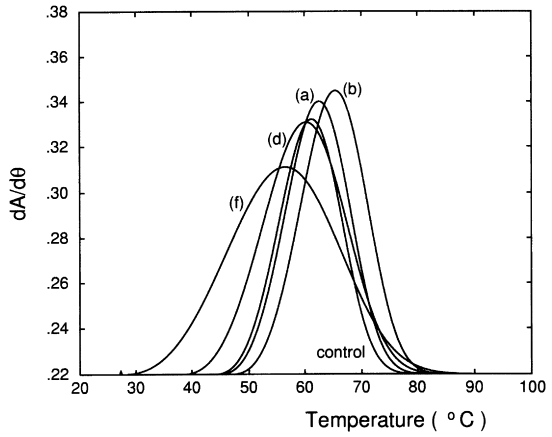

Fig. 3. First derivaties of the best-fit melting curves for the non-irradiated DNA samples (control) and DNA samples irradiated with 1.6 (a), 3.9 (b), 37 (d) and 150 (f) Gy of γ-rays from a ^{60}Co source.

1. The maximum of the first derivatives is shifted to higher temperatures for the samples exposed to *low* doses (radiation-induced thermal stability) and for the samples exposed to higher doses the decrease of stability is confirmed through the significant shifting of the maximum to *lower* temperatures.

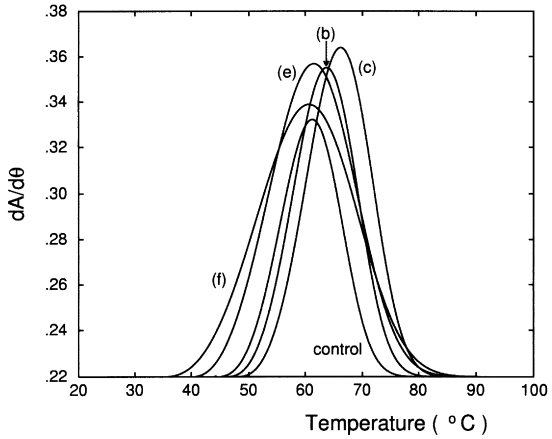

Fig. 4. First derivatives of the best-fit melting curves for the non-irradiated DNA samples (control) and DNA samples irradiated with 4 (b), 12 (c), 56 (e) and 100 (f) Gy of α-particles from ^{241}Am source.

2. The full width at half maximum height (FWHM) for the samples exposed to *low* doses, shows only a slight increase compared with the control in contrast to the samples exposed to *high* doses where a significant increase is revealed. The increase at FWHM is consistent with the presence of a larger variety of DNA segments in the irradiated samples. The slight increase at *low* doses implies no statistically important degradation of the DNA molecules, something that is compatible with the mean MW's analysis results presented in Section 3.2.

In the melting curves presented in Figs. 1 and 2 one observes that at *low* doses the total hyperchromicity of the samples is slightly higher compared to that of the control while at higher doses it is relatively smaller. This observation was also verified by the estimation of the model parameter A_u (total hyperchromicity) which shows the same dual behavior at the *low* and *high* dose region, respectively (data not shown). A similar behavior was found by Ward and Urist [10] for γ-irradiated polynucleotides. They have attributed the increase of hyperchromicity at *low* doses to the base shielding in the regular B-DNA native form. Only when *high* doses of γ-irradiation cause a degradation of the double helix the hyperchromicity starts to decrease. Our results at *low* doses could also be explained by a positive effect on DNA base stacking. This hypothesis is compatible with a previous work suggesting that at *low* doses an intermediate B-DNA form may exist [31]. This intermediate form of the double helix would be characterised only by local changes in the B-DNA structure and not by an overall degradation which occurs only at *high* doses.

3.2. Molecular size analysis

The fluorescence intensity profiles of samples exposed to *low* and *high* doses of α- and γ-irradiation are presented in Fig. 5 and Fig. 6, respectively, as found from PFGE analysis. For the samples exposed to *low* doses only a slight widening of the DNA distributions can be observed. At higher doses, a significant widening of the distributions is observed due to the existence of a wide variety of DNA fragments as a result of the radiation-induced double strand breaks. These findings are compatible with that of the melting analysis (presented in Section 3.1) and all of them suggest that at *low* doses, irradiation does not affect significantly B-DNA structure. In addition, the insignificant (statistically) number of molecules with reduced size (in respect to the control) at *low* doses and the significant (statistically) number of molecules of higher size (in respect to the control) led to an increased mean apparent MW for the samples exposed to *low* doses of α- and γ-irradiation. The estimated apparent MWs from the electrophoretic mobility are presented in Fig. 7 for both α- and γ-irradiation. The observed relative increase at *low* doses might be related to the formation of higher sized DNA molecules due to DNA–DNA interactions of nearby strands. As it is known [32], nicked DNA molecules are remarkably efficient in capturing complementary DNA sequences at dilute concentrations via ionic interactions. On a different approach, the observed decrease of the electrophoretic mobility might also be related to the different mobility of the samples exposed to low doses due to moderate radiation-induced conformational changes. It is known from several studies that DNA molecules with slightly different conformations migrate quite differently in polyacrylamide gels [33]. This conformation-dependent change of mobility under a constant external applied field (standard agarose gel electrophoresis) might be also occurring under the pulsed field applied in PFGE.

3.3. Thermal stability

By differentiating the fit melting curves one can estimate the T_M for each sample as the temperature at which the first derivative (see Figs. 3 and 4) is maximum. The estimated mean T_M values for all samples exposed to *low* and *high* doses of α- and γ-irradiation are shown in Fig. 8. The presented values are corrected for fragment size effect according to [17] and the presented error bars correspond to S.D. of the mean values. The T_M values were also determined in the classical

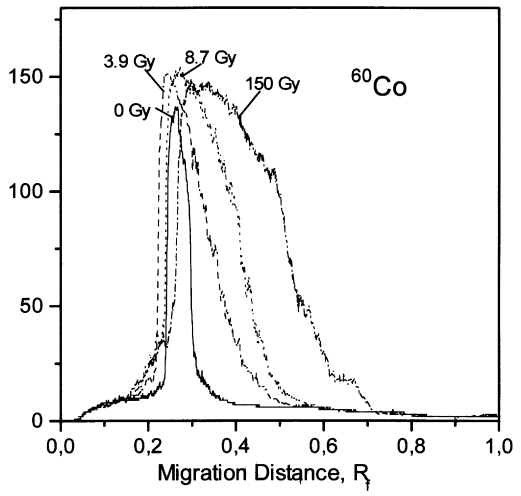

Fig. 5. The distribution of fluorescent intensity on a PFGE gel stained with ethidium bromide for four representative DNA samples exposed to γ-rays from a ^{60}Co source, as a function of the migration distance. Control (0 Gy).

way, as the temperature at which 50% of the maximum hyperchromicity is observed [1]. These data are not shown since they were found to lie within the standard error of the presented mean values.

Figs. 1, 2 and 7 reveal the presence of two

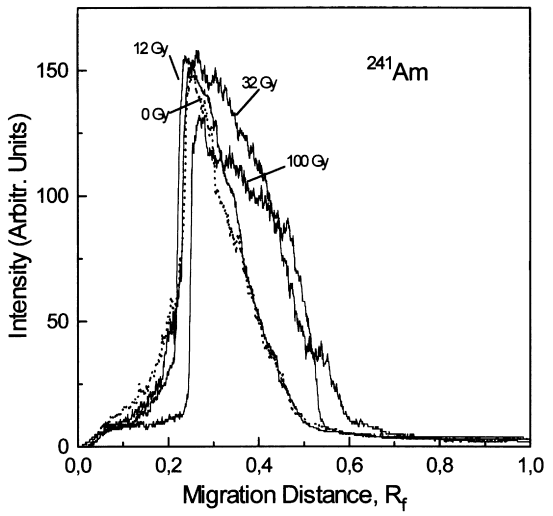

Fig. 6. The distribution of fluorescent intensity on a PFGE gel stained with ethidium bromide for four representative DNA samples exposed to α-particles from an ^{241}Am source, as a function of the migration distance. Control (0 Gy).

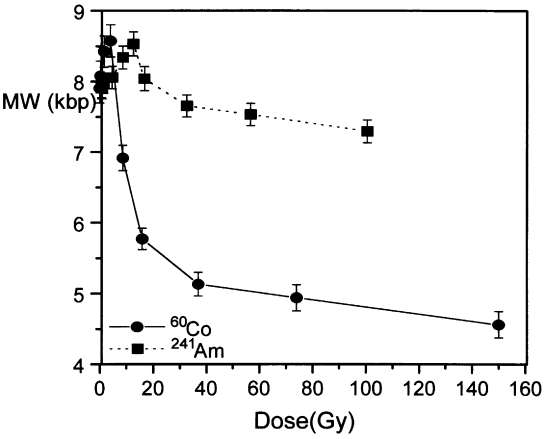

Fig. 7. The estimated mean apparent MW values (in kilobase pairs) based on PFGE as a fimction of dose, for samples exposed to γ- and α-irradiation from a ^{60}Co and ^{241}Am source, respectively.

different dose regions as far as the 'melting' characteristics and electrophoretic mobility of the samples are concerned, the *low* and the *high* dose region. The samples exposed to *low* doses for both α- and γ-radiation show an enhanced stability towards the control samples and the samples exposed to *high* doses while the variation of mean apparent MWs as the function of dose shows similar behaviour, i.e. an increase at *low* doses followed by a gradual decrease at higher doses.

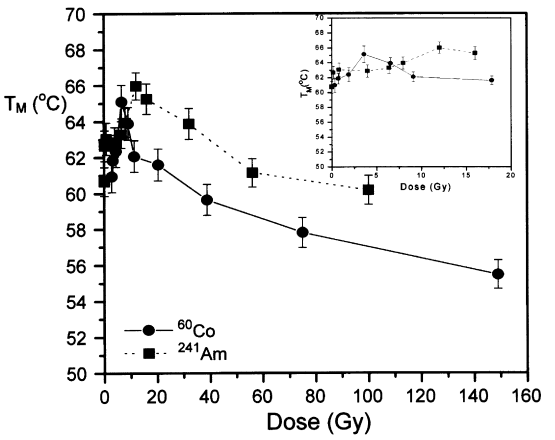

Fig. 8. The estimated mean melting temperatures T_Ms as a function of dose, for samples exposed to γ- and α-irradiation from a ^{60}Co and ^{241}Am source, respectively. Inset: A magnification of the *low* dose region.

Comparing Figs. 7 and 8 one observes that the range of *low* dose region is different for α- and γ-radiation and a factor of ~5–6 seems to characterise the higher extension for the case of α-particles. The transition from the *low* to the *high* dose region occurs for both types of radiations when the number of SSBs/DNA molecule (and the effective DSBs) increase to a level that produces an overall instability (T_M and MW values start to decrease *below* those of the control). Data in literature suggest a 4–10-fold higher SSB yield/Gy for γ-rays towards α-particles, a value which varies according to irradiation conditions and type of DNA (plasmid or mammalian) [30,34]. This number is compatible with the differences between the ranges of *low* dose regions for α- and γ-radiation observed here. Exposure to *low* doses of α- (0–32 Gy) and γ- (0–6 Gy) irradiation is expected [30] to create about 1 SSB (or less) per calf thymus DNA molecule in the moderate scavenging conditions of our experiments, i.e. at scavenging capacities $\sim 12.5 \times 10^6$ s^{-1} due to DNA and $\sim 6 \times 10^4$ s^{-1} due to citrate taking $k(OH^{\cdot} \pm \text{Citrate}) = 4.1 \times 10^7$ l/mol and $k(OH^{\cdot} \pm$ DNA per nucleotide subunit$) = 2.5 \times 10^8$ l/mol. The above fact implies that at the *low* dose region, nicked DNA molecules mostly exist with maximum 1–2 SSBs at their sequence. Many studies [33,35,36] with calf thymus DNA or short DNA duplexes suggest that, in general, nicks (altered bases or sugars and/or SSBs) do not either affect the flexibility or significantly alter the overall conformation of the DNA molecule whereas a more extended interruption does. In the case of a nick changes in structure are small and localised around the nick. The nicked DNA forms seem to have conformations very close to the B-DNA form with only small local differences relative to the native B-form, if their number is not high. Melting studies [36] indicate that nicked DNA molecules can also exhibit 'melting' characteristics identical to those of native molecules. The enhanced thermal stability that we found for the nicked molecules (*low* doses) is probably related to the already verified [32,37] increased ability of such molecules to form base stacking interactions with other molecules in the solution.

3.4. Interpretation of the data based on the model parameters

In Fig. 9 the average relative base pair disruption per unit increase in temperature ($N+1$ root of c) as described in [1], is plotted as a function of dose for samples exposed to both α- and γ-irradiation. According to the above model, N is related to the possible paths through which energy is conducted along the DNA molecule. In the same figure, we observe that irradiation with *low* doses facilitates the disruption of DNA base pairs although it increases thermal stability. The maximum disruption is always observed for the samples, which show the higher thermal stability (Fig. 8). The fact that at *low* doses the disruption increases is indicative of the widely accepted idea that the conformation of intact DNA shields the bases inside the double helix from radical attack [12,38]. This protection decreases as the number of SSBs and DSBs increases, resulting in the 'unzipping' of the helix and the onset of denaturation [14]. As the radiation-induced denaturation increases at higher doses, the percentage of bases, which are exposed to the solution, increases dramatically. Taking into account the well known high reaction rate constants of all DNA bases [39] with $^{\cdot}OH$ radicals, as soon as they are exposed to

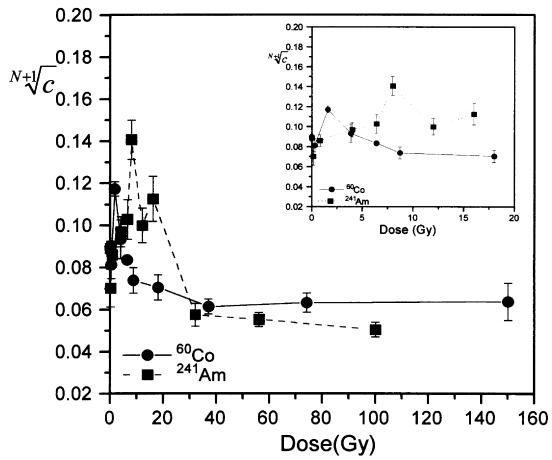

Fig. 9. The mean values of the parameter $N+1$ root of c as a function of dose, calculated using Eq. (1), for samples exposed to γ- and α-radiation from a ^{60}Co and ^{241}Am source, respectively. Inset: A magnification of the *low* dose region.

a relative high dose (e.g. approx. 30–10 Gy for α and γ-irradiation as seen in Fig. 9) the destruction very quickly reaches a saturation point. When thermodynamic parameters were estimated in our laboratory [40] by applying inverse gas chromatography, it was found that the region of 0–40 Gy of γ-irradiation at different concentration conditions (4.5×10^{-5} M in DNA-P), is characterised by a high efficiency in structural alteration of the DNA molecules with a tendency for saturation at higher doses. However, in the above mentioned work, no data exist for the *low* dose region of 0–6 Gy. We believe that, the up to now unknown dependence of the $N+1$ root of c on concentration and radiation dose, starts to reveal itself and two tendencies seem to be apparent from the present results and under the present conditions. The first is that the saturation and minimization region seems to occur at lower doses with increasing DNA concentration and the second is that between these specific low and high LET radiations the saturation region occurs earlier for the high LET radiation (α-particles). It must be pointed out that the value of $N+1$ root of c is higher for α-particles than γ-irradiation (at the dose of 12 Gy, where the higher thermal stability is observed). This may explain why the saturation region occurs at lower doses for this type of radiation, considering also the earlier discussion about the opening of the helix resulting in the exposure of bases to solution and the important role of different stacking interactions (and DNA conformations) for these two types of radiation. It seems that the absolute number of SSBs (which is higher for γ-irradiation) is not the only factor which regulates exposure of the DNA bases to the bulk solution.

The dose region at which the saturation for the disruption of base pairs occurs (see Fig. 9) coincides with the dose region where the parameter N is maximised as it can be seen in Fig. 10, where the variation of N with dose is plotted for α- and γ-irradiation, respectively. At the *low*-dose region the values of N, which according to the proposed model are related to the possible pathways for energy transduction across the DNA helix, show a tendency to decrease with dose. In passing from the *low* dose region to the *high* one, the exponent

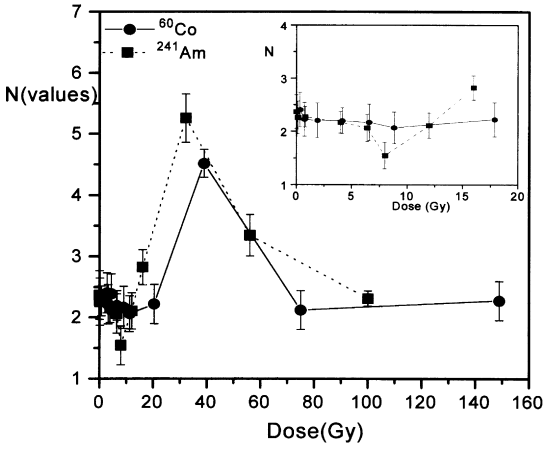

Fig. 10. The mean values of the parameter N as a function of dose, calculated using Eq. (1), for samples exposed to γ- and α-radiation from a ^{60}Co and ^{241}Am source, respectively. Inset: A magnification of the *low* dose region.

N increases significantly (as already described) and for higher doses it decreases again to the initial levels. This multi-phase behaviour of N is highly related to the dose-dependence of base pair disruption (described above) and the changes in the molecular size (Fig. 7). To be more specific, at *low* doses, as it is stated above, ionising radiation is quite effective in the base pair disruption mainly through localised opening (and denaturation) of the helix without reducing the size of the DNA molecule. This local disruption of base pair stacking will disrupt the flow of thermal energy along the long axis of DNA through solitary wave excitations (see Section 1). The remaining modes of thermal energy transfer are inaccessible [1,41]. Therefore the disruption of the thermal energy flow would result in decreasing values of N as found for the nicked molecules for the samples exposed to *low* doses. The discussed difficulties in the propagation of energy across the molecule may explain the higher thermal energy quantities required for the nicked molecules to denaturate. Exposure to higher doses of irradiation leads to the increase of N as suggested by Kalfas et al. [1]. This is probably related to the increasing production of DSBs as revealed in Fig. 7 through the decrease of MW for higher doses. The production of DSBs tends to form DNA fragments of smaller

size, resulting in a higher surface to volume ratio for the fragments as compared to the intact DNA. Therefore, N is expected to show a tendency to increase again due to an increased conduction of thermal energy from the solution to the DNA. This increase is also verified in this work. This facilitation of the energy propagation through the smaller size segments is minimised at the *high* dose region due to the extensive damage of the specific segments which significantly perturbs energy propagation again, resulting in the decrease of N in an asymptotical way. The specific asymptotical behaviour is directly related to the similar variation of MW with dose at the same dose regions (Fig. 7). As seen in Fig. 7, the decrease of size tends asymptotically towards a *lower* constant value, i.e. the number of effective DSBs which lead to further fragmentation of the DNA molecules is minimised.

In Fig. 11 the variation of threshold temperature θ_0 with dose can be seen for each case of radiation or concentration presented in the previous Figs. 8 and 9. The temperature θ_0, is a measure of the remaining (after irradiation) difference in the stacking free energy between the intact and the open states. The higher the stacking of the helix the higher the temperature θ_0, and of course the higher the amount of thermal energy to pass from the native to the denaturated

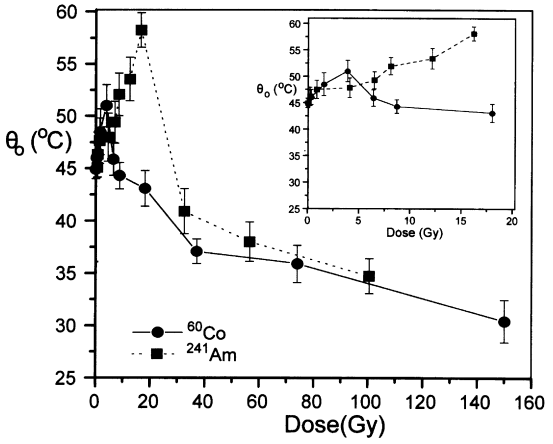

Fig. 11. The mean values of the parameter θ_0, as a function of dose, calculated using Eq. (1), for samples exposed to γ- and α-radiation from a ^{60}Co and ^{241}Am source, respectively. Inset: A magnification of the *low* dose region.

form of the DNA. One can say that, this parameter is analogous to the overall stacking existing in the DNA molecule in the solution where the measurement takes place. The results show (as expected from all the previous analysis) that θ_0 (and stacking) is maximised for the samples exposed to *low* doses. This finding, according to our opinion, is very crucial because it strengthens our suggestion of a more positive (in relation to the native DNA) total base stacking existing for the nicked molecules of *low* doses. Based on Fig. 11 one can see that the decrease of stacking for doses higher than 50 Gy for γ-irradiation does not seem to reach a saturation point like in the case of α-particles. This behaviour is in good agreement with the variation of the overall stability (T_M) with dose and type of radiation seen in Fig. 8. The known higher efficiency of γ-rays as compared to α-particles to produce DNA damage [34,43] is mirrored in these two figures and also in Fig. 7 where it can be seen that at the same dose region the size of γ-irradiated samples is significantly *lower* for doses higher than 20 Gy. The higher fragmentation of the γ-irradiated samples perturbs more severely and more persistently the overall stability and stacking as it can be concluded by the continuous decrease of the T_M and θ_0 values. At last, the fact that in the case of the $N+1$ root of c variation with dose we do find a saturation region in all cases, is indicative that the overall DNA stability and base stacking do not depend only on the number of disrupted base pairs i.e. the T_M values are not linearly related to the changes in the relative maximum numbers of disrupted base pairs, a conclusion also reached by Kalfas et al. [1].

4. Conclusions

In this work, we test the energy propagation model proposed by Kalfas et al. [1] for the thermal transition of a DNA macromolecule which was exposed to two different types of ionising radiation and under dilferent irradiation conditions. We gave special attention to the region of *low* doses in order to enlight this region which from the early 1960s [12,18] appears to be a

region characterised by a non-linear behaviour of several parameters such as the radiation-induced loss in hyperchromicity and the thermal denaturation of the DNA double helix. These early suggested ideas about the importance of the post-irradiation conformational changes of the DNA helix in determining radiation damage and the observed non-linearity of DNA damage with dose at the region of *low* doses can now be understood in the framework of the energy propagation model [1] and is probably related to the influence of the localised damages in the ability of the molecule to interact with neighbouring molecules via stacking and in the propagation of thermal energy across the molecule.

No specific mathematical correlation between the parameters N and $N+1$ root of c of the model and radiation dose has yet been attempted. In the present work, we are able to give the general trend of these parameters with dose and irradiation conditions. Furthermore, this is the first attempt to correlate the effects of ionising radiation of different quality (low and high LET radiations) with the propagation of thermal energy, based on our results and the existing literature on the differences between the two applied radiations.

In conclusion, the proposed theory of Kalfas et al. [1] gives a very good quantitative and qualitative description of the radiation-induced perturbations in the thermal transition of the DNA macromolecule especially in the region of *low* doses where an enhanced stability was found. The experimental and theoretical analysis leads to the conclusion that the samples exposed to *low* doses have no severe structural alterations towards the native samples. The significance of these suggested localised perturbations which were found to affect negatively the energy *flow* across the DNA molecule, may affect the recognition of the DNA by proteins and may affect the packaging of DNA in nucleosomes within the cell as also suggested by other studies [44].

Acknowledgements

The authors wish to express their sincere thanks to Dr V. Sophianopoulou and Dr M. Spotheim Maurizot for all the helpful discussions and suggestions. This work was partially supported by the EEC Grant F14P-CT95-0011 and 1088/95 Grant of the Greek General Secretariat and Technology.

Appendix A: With the permission of the authors, the highlights of the energy propagation model of Kalfas et al. [1] are given below

As in all theoretical approaches, DNA is considered as a quasi one-dimensional lattice composed of N base pair units. Under ordinary conditions, it forms a double helix (B form). This double-stranded structure is held together by hydrogen bonds between complementary base pairs (A-T or G-C) and stacking (hydrophobic) interactions between nearest neighbour bases on same strands. When the excitation modes of an individual nucleotide are considered, it is seen that the energy required for a transition between the two lowest S_0 and S_1 states is of the order of 80 kcal mol^{-1}, while transitions between vibrational levels require energies of the order of 10 kcal mol^{-1}. Therefore, thermal energies at room temperature could only induce transitions between rotational states of the individual nucleotides since the spacing of their energy levels is of the order of 1 kcal mol^{-1}. In addition, the 'stacking potential' will allow energy to be stored in the form of vibrations between nearest neighbour bases at same strands. However, it is difficult to visualise that this part of the internal (thermal) energy of such a structure could be stored in the form of coherent vibrations covering the whole length of the formation constituting a DNA molecule. As more likely, local coherent vibrations covering a few tens or hundreds of base pairs would prevail. Each group of coherently vibrating stacked base pairs along the DNA axis can constitute a 'rod'. An increase in temperature and, therefore in internal energy, will result in an increase of the vibrating amplitudes, eventually leading to unstacking and a subsequent weakening of the hydrogen bonding between the complementary base pairs. This, will in turn, facilitate the disruption of

the hydrogen bonds leading to the denaturation or melting of DNA, forming single stranded chains.

In the framework of this overall picture, one can attempt to develop a quantitative description of the behaviour of DNA under varying external conditions, such as temperature, or when subjecting DNA to any form of ionising radiation, such as gamma rays.

One of the most frequently used methods to investigate the melting transition in DNA is the measurement of the variation in the UV absorbance of a dilute DNA solution as a function of increasing temperature. The basic assumption of the *cited* theoretical description is that the observed hyperchromicity (i.e. increased UV absorbance) in the melting transition of DNA is directly proportional to the number of disrupted base pairs. Thus, the UV absorbance and, consequently, the number of disrupted base pairs can be expressed in terms of a temperature function $y = f(\theta)$. In addition, it is assumed that the temperature variation of y related to base pairs disruption must depend on:

- The number of available stacked base pairs, as expressed by the term $k - y$, where k is the total number of base pairs;
- The temperature of the solution θ; and
- The difference in the stacking free energy between the intact and the open states for which a threshold temperature θ_0, can be assigned.

The functional form of the temperature dependence can be derived from a reasoning based on the energy flow from the aqueous solution to any site on DNA and then along the overall structure of DNA. From the definition of θ_0, one can suggest that the energy which propagates along the overall structure and is available for base pair disruption, must depend on $\theta - \theta_0$. It is then reasonable to assume that the base pair disruption is a power function of $\theta - \theta_0$ (i.e. it has the form of $(\theta - \theta_0)^N$) where the exponent N is related to the possible paths along which energy is conducted. The power form is readily understood, if each such path is considered as having an independent contribution, while the overall effect is the composite result. Bearing in mind that it is generally assumed that DNA can be viewed as a quasi one-dimensional lattice, N must be relatively small, which is in contrast to the case of a crystalline structure of any solid where N must tend to infinity. Thus, in this model a special importance is assigned to the variation in the value of N when associated structural variations are studied.

Expressing the above reasoning in quantitative form, for $\theta > \theta_0$,

$$\frac{dy}{d\theta} = c \cdot (\theta - \theta_0)^N \cdot (k - y) \tag{A.1}$$

where c is a proportionality constant.

By integrating

$$-\ln(k - y) = \left[c(\theta - \theta_0)^{N+1}/N + 1 \right] + C^{st} \tag{A.2}$$

$$k - y = h \cdot e^{-[c(\theta - \theta_0)^{N+1}]/(N+1)} \tag{A.3}$$

Making the substitution $k = g + h$

$$y = g + h \cdot (1 - e^{-[c(\theta - \theta_0)^{N+1}]/(N+1)}) \tag{A.4}$$

where the physical meaning of g and h is derived from the assumption that absorbance can be used in place of the number of paired and disrupted bases, respectively. Consequently, the expression can be written as:

$$A(\theta) = A_{st} + A_u \cdot \{1 - e^{-[c(\theta - \theta_0)^{N+1}]/(N+1)}\}$$

$$\text{for } \theta > \theta_0 \tag{A.5}$$

$$A(\theta) = A_{st} \quad \text{for } \theta < \theta_0 \tag{A.5a}$$

where, A_{st}, is the UV absorbance of the tight DNA helix, and A_u is the hyperchromicity (i.e. the increase in absorbance of a totally denatured DNA molecule). The subscripts '*st*' and '*u*' stand for 'stacked' and 'unstacked', respectively.

Working backwards, Eq. (A.1) can be re-written by differentiating Eq. (A.4) in the form:

$$\frac{dy}{d\theta} = h \cdot c \cdot e^{-[c(\theta-\theta_0)^{N+1}]/(N+1)} \cdot (\theta-\theta_0)^N \qquad (A.6)$$

One can define the melting point of DNA either as the temperature at the maximum slope in the melting curve (i.e. absorbance vs. temperature) or as the temperature for which the population of the stacked base pairs is reduced to 50% to its original value. The first definition, [by equating to zero after differentiating Eq. (A.6)] leads to

$$T_m = \theta_0 + \sqrt[N+1]{\frac{N}{c}} \qquad (A.7)$$

while the second (which is traditionally used), after equating the exponential term in Eq. (A.6) to 0.5 leads to

$$T_m = \theta_0 + \sqrt[N+1]{\frac{(N+1)\cdot \ln 2}{c}} \qquad (A.8)$$

The two slightly different definitions should not be a source of confusion. In reality, their difference is less than a few percent. The first definition has the advantage of a graphical representation in a $dy/d\theta$ vs. θ plot, while the second is the traditionally accepted definition and is essentially model independent.

References

[1] C.A. Kalfas, G.K. Loukakis, A.G. Georgakilas, E.G. Sideris, A. Anagnostopoulou-Konsta, J. Biol. Syst. 4 (1996) 405.

[2] J. Kiefer, Biological Radiation Effects, Springer-Verlag, Berlin, 1990.

[3] J.R. Milligan, J.A. Aguilera, C.C.L. Wu, J.Y.-Y. Ng, J.F. Ward, Radiat. Res. 145 (1996) 442.

[4] C. von Sonntaq, The Chemical Basis of Radiation Biology, Taylor and Francis, London, 1987.

[5] K. Washino, W. Schnabel, Die Makromolekulare Chem. 6 (1982) 697.

[6] J. Heilmann, G. Taucher-Scholz, G. Kraft, Int. J. Radiat. Biol. 68 (1995) 153.

[7] C.M. Wheeler, Changes in the secondary and tertiary structures of DNA after irradiation, in: J. Hutterman, W. Kohnlein, R. Teoule, A.J. Bertinchamps (Eds.), Effects of Ionizing Radiation on DNA, Springer-Verlag, New York, 1978, p. 227.

[8] J. Petruska, F.M. Goodman, J. Biol. Chem. 6 (1995) 746.

[9] A. Sarai, J. Mazur, R. Nussinov, L.R. Jernigan, Biochemistry 27 (1988) 8498.

[10] J.F. Ward, M.M. Urist, Int. J. Rad. Biol. 12 (1967) 209.

[11] F.N. Hayes, D.E. Hoard, U. Hollstein, W.B. Goad, C. Delisi, Biophys. Chem. 8 (1978) 123.

[12] A. Rafi, J.J. Weiss, C.M. Wheeler, Biochim. Biophys. Acta 169 (1968) 230.

[13] J.R. Milligan, J.A. Aguilera, J.F. Ward, Rad. Res. 63 (1993) 151.

[14] G. Scholes, J.F. Ward, J.J. Weiss, J. Mol. Biol. 2 (1960) 379.

[15] J. Marmur, P. Doty, J. Mol. Biol. 5 (1962) 109.

[16] C. Schildkraut, S. Lifson, Biopolymers 3 (1965) 195.

[17] J.R. Britten, E.D. Graham, R.B. Neufeld, Analysis of repeating DNA sequences by reassiociation, in: L. Grossman, K. Moldave (Eds.), Methods in Enzymology, XXIX, Academic Press, New York and London, 1974, p. 363.

[18] U. Hagen, R. Wild, Strahlentherapie 124 (1964) 275.

[19] A.A. Rafi, C.M. Wheeler, Int. J. Rad. Biol. 24 (1973) 321.

[20] D.F. Uyesugi, C.N. Trumbore, Int. J. Rad. Biol. 44 (1983) 627.

[21] C.N. Trumbore, Y.N. Myers, C.K. Hyde, R.D. Hudson, C.N. Rhodes, J.K. Masselink, Int. J. Radiat. Biol. 66 (1994) 479.

[22] A.G. Georgakilas, K.S. Haveles, L.H. Margaritis, L. Sakelliou, E.G. Sideris, Radiat. Res. 148 (1997) 503.

[23] G. Gotoh, Adv. Biophys. 16 (1983) 1.

[24] R.M. Wartell, A.S. Benight, Phys. Reports 126 (1985) 67.

[25] G. Edwards, Y. Guangtao, J. Tribble, Phys. Rev. 45 (1992) 8344.

[26] T. Dauxois, M. Peyrard, R.A. Bishop, Physica D 66 (1993) 35.

[27] F. James, M. Roos, Comput. Phys. Comm. 10 (1975) 343.

[28] G. Zarris, A. Georgakilas, L. Sakelliou, K. Sarigiannis, E.G. Sideris, Radiat. Measurements 29 (1999) 611.

[29] A.G. Georgakilas, A.A. Konsta, K.S. Haveles, E.G. Sideris, IEEE Trans. Dielectr. Electr. Insul. Society 5 (1999) 26.

[30] R. Roots, W. Holley, A. Chatterjee, M. Irizarry, G. Kraft, Int. J. Radiat. Biol. 58 (1990) 55.

[31] M. Vorlickova, E. Palecek, Int. J. Radiat. Biol. 26 (1974) 363.

[32] J.M. Lane, T. Paner, I. Kashin, D.B. Faldasz, B. Li, J.F. Gallo, S.A. Benight, Nucleic Acids Res. 3 (1997) 611.

[33] A. Bonicontro, M. Matzeu, F. Mazzei, A. Minorpio, F. Pedone, BBA 1171 (1993) 288.

[34] G.D.D. Jones, J.R. Milligan, J.F. Ward, P.M. Calabro-Jones, J.A. Aguilera, Radiat. Res. 14 (1993) 190.

[35] J.B. Hays, B.H. Zimm, J. Mol. Biol. 48 (1970) 297.

[36] E.A. Snowden-Ifft, D.E. Wemmer, Biochemistry 29 (1990) 6017.

[37] C. Herskind, Int. J. Rad. Biol. 52 (1987) 565.
[38] K. Sailer, S. Viaggi, M. Nusse, Int. J. Radiat. Biol. 58 (1990) 55.
[39] V. Michalik, M. Spotheim-Maurizot, M. Charlier, J. Biomol. Struct. Dyn. 6 (1995) 565.
[40] G. Loukakis, E.G. Sideris, C.A. Kalfas, B.E. Mazomenos, A. Anagnostopoulou-Konsta, Topics Molecular Org. Eng. 8 (1991) 44.
[41] C.R. Cantor, P. Schimmel, Biophysical Chemistry, W.H Freeman and Co, New York, 1980.
[42] A.G. Georgakilas, K.S. Haveles, A.A. Konsta, E.G. Sideris, IEEE Dielectr. Electr. Insul. Society ISE 9 (1996) 747.
[43] P.S. Hodgkins, P. O'Neill, D. Stevens, P.M. Fairman, Radiat. Res. 146 (1996) 660.
[44] J.Y. Kao, I. Goljer, T.A. Phan, P.H. Bolton, J. Biol. Chem. 268 (1993) 17787.